

absorption constants in an absorption process where allowance has not been made for the reflection loss.

### SUMMARY

The exciton absorption of KCl and NaCl observed in reflected light would seem to make useful this method of investigating the absorptions of single crystals as opposed to transmission techniques through uncertain thin evaporated films of the crystal salt.

### ACKNOWLEDGMENTS

It is a pleasure to acknowledge the help of various people in the work, including particularly helpful discussions with A. W. Overhauser, J. A. Krumshansl, L. G. Parratt, and E. L. Jossem. Mr. J. W. Taylor has aided in some of the measurements. Thanks are also due to Mr. J. P. Gilvey for help in supplying and handling liquid helium.

## Magnetic Structures in Copper-Manganese Alloys\*

DAVID MENEGHETTI† AND S. S. SIDHU  
Argonne National Laboratory, Lemont, Illinois  
(Received September 24, 1956)

A neutron diffraction study of a series of substitutional solid solutions up to 85 atomic percent manganese in copper has shown that at about 13 atomic percent manganese, a broad intensity maximum appears in the region of (100) reflection of the face-centered cubic pattern of copper. A correlation of this maximum with the magnetic attraction of the specimens indicates that it is at least in part due to short-range magnetic order. Its intensity decreases at compositions greater than 50 atomic percent manganese. Above 69 atomic percent manganese an antiferromagnetic structure is observed and is interpreted as due to an antiferromagnetic coupling between manganese atoms as the manganese concentration becomes predominant.

### I. INTRODUCTION

THE copper-manganese alloy system is particularly suited for study by neutron diffraction. In the continuous substitutional solid solutions<sup>1-3</sup> from copper-rich to manganese-rich phases, manganese atoms have a predominance of unlike and like atoms, respectively, as neighbors. Copper being diamagnetic and manganese paramagnetic it is of interest to determine if the magnetic moments of the manganese atoms and their alignments are affected by such spatial arrangements of the two kinds of atoms. The presence or absence of magnetic or antiferromagnetic structures and the dependence of paramagnetic scattering upon composition may be observed. In addition, as the coherent neutron scattering amplitudes of copper and manganese nuclei are opposite in sign,<sup>4</sup> superstructure lines due to atomic ordering in the alloys, if present, should be observed much more readily<sup>5</sup> than with x-rays<sup>6</sup> for which the atomic scattering factors are of nearly the same magnitude.

\* Work performed under the auspices of the U. S. Atomic Energy Commission.

† Part of a thesis presented by D. Meneghetti in partial fulfillment of the requirements for the degree of Doctor of Philosophy at the Illinois Institute of Technology, 1954.

<sup>1</sup> E. Persson, *Z. physik. Chem.* **B9**, 25 (1930).

<sup>2</sup> Dean, Long, Graham, Potter, and Hayes, *Trans. Am. Soc. Metals* **34**, 443 (1945).

<sup>3</sup> Dean, Potter, Long, and Huber, *Trans. Am. Soc. Metals* **34**, 465 (1945).

<sup>4</sup> E. O. Wollan and C. G. Shull, *Phys. Rev.* **73**, 830 (1948).

<sup>5</sup> C. G. Shull and E. O. Wollan, *Phys. Rev.* **81**, 527 (1951).

<sup>6</sup> L. D. Ellsworth and F. C. Blake, *J. Appl. Phys.* **15**, 507 (1944).

The magnetic susceptibility of the copper-manganese system has been reported<sup>7</sup> as having a maximum in the region of 22 atomic percent manganese. At liquid nitrogen temperature this maximum increased by a factor of about seven; whereas, only a small increase occurred in the remainder of the curve. Since neutrons can be coherently scattered by magnetic structures,<sup>8</sup> the neutron diffraction patterns may enable the reported magnetic susceptibility characteristics to be interpreted in terms of orderings of atomic magnetic moments.

### II. EXPERIMENTAL PROCEDURE

The chemical and x-ray analyses of the samples used in this investigation are given in Table I.

TABLE I. Chemical and x-ray analyses of the alloys.

Sample	Atomic percent		Phase	Lattice parameters	
	Mn	Cu		$a_0$	$c_0$
Cu		100	f.c.c. <sup>a</sup>	3.61 Å	
11 Mn-89 Cu	10.5	89.4		3.64 Å	
13 Mn-87 Cu <sup>a</sup>	12.7	87.2		3.65 Å	
18 Mn-82 Cu	17.5	82.5		3.66 Å	
33 Mn-67 Cu <sup>a</sup>	33.2	66.9		3.72 Å	
48 Mn-52 Cu	47.7	52.3		3.75 Å	
48 Mn-52 Cu <sup>b</sup>	48.4	51.7		3.75 Å	
69 Mn-31 Cu	69.0	31.0		3.75 Å	
75 Mn-25 Cu	74.6	25.4	f.c.t.		
85 Mn-15 Cu	85.1	14.9	f.c.t.	3.76 Å	3.64 Å

<sup>a</sup> Commercial samples.

<sup>b</sup> Quenched sample.

<sup>c</sup> f.c.c.: face-centered cubic; f.c.t.: face-centered tetragonal.

<sup>7</sup> S. Valentiner and G. Becker, *Z. Physik* **80**, 735 (1933).

<sup>8</sup> Shull, Strauser, and Wollan, *Phys. Rev.* **83**, 333 (1951).

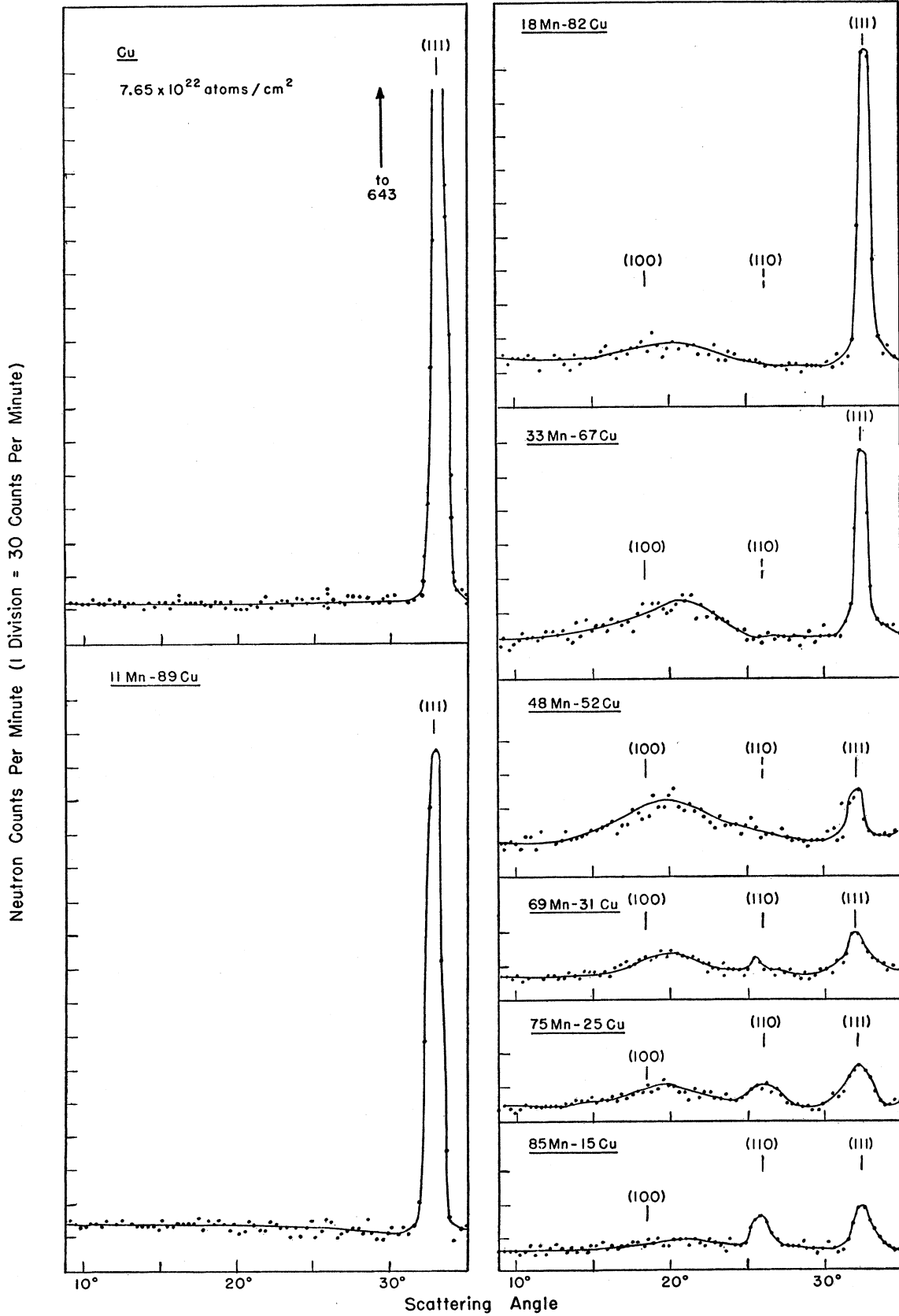


FIG. 1. Low-angle portions of neutron diffraction patterns of copper-manganese alloys.

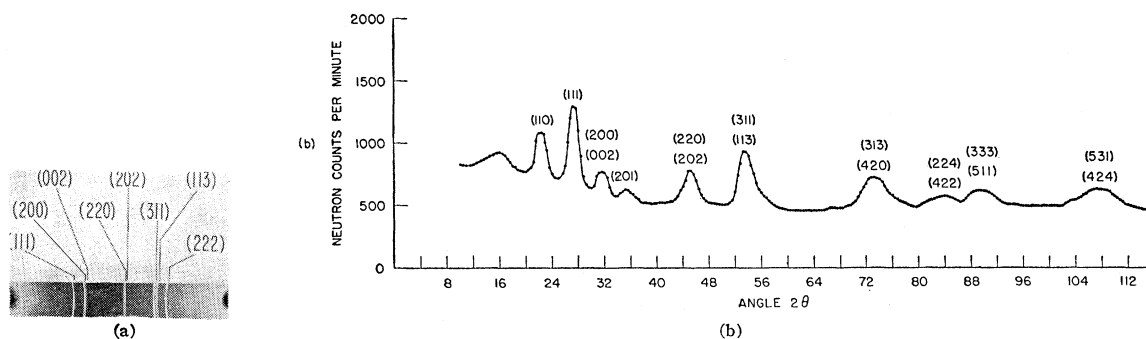


FIG. 2. Diffraction patterns of 85% Mn-15% Cu. (a) X-ray filtered Fe  $K_{\alpha}$  radiation, camera diameter 114.6 mm. (b) Neutron,  $\lambda=1.01$  Å.

The laboratory-prepared samples were fused in alundum crucibles in a vacuum induction furnace at 1300°C for 20 min and then cooled to room temperature in the furnace. Argon gas at a pressure of five inches of mercury was maintained in the furnace to prevent loss of manganese in the manganese-rich alloys. After cooling, the crucibles were broken and the samples machined into disks 2 in. in diameter and  $\frac{3}{8}$  in. thick.

Except where otherwise indicated, the neutron diffraction patterns were observed with neutrons of wavelength 1.19 Å, a 1 in.  $\times$  2 in. beam area, and collimation such as to give a 1° angular resolution of the diffraction patterns.

The relative magnetic attractions of the samples were determined by measuring the maximum horizontal displacement produced by a permanent magnet of about 2000-gauss field strength upon each sample when suspended vertically by a string between the poles of the magnet.

### III. RESULTS AND DISCUSSION

An x-ray diffraction analysis of the copper-manganese alloys studied here showed the usual patterns of the face-centered cubic and the face-centered tetragonal

structures observed in this system. The neutron diffraction patterns of the same samples, however, exhibited in addition (1) a broad maximum in the region of (100) reflection over a large range of intermediate alloy compositions and (2) additional diffraction lines at (110) and (201) positions in the manganese-rich alloys. The low-angle regions of the neutron patterns for the series of alloys normalized to the same number of atoms per unit area of sample are plotted to scale in Fig. 1. It is seen that as the concentration of manganese atoms in copper increases there is, at first, an increase in the diffuse background. This is followed by the formation of the broad reflection. At higher concentrations the intensity of the diffuse background as well as of the broad reflection decreases and the reflections (110) and (201) appear as shown on Fig. 2.<sup>9</sup> There is, of course, a decrease in the intensities of the normal lattice reflections, as exemplified by the decrease in the (111) reflection, since the neutron scattering amplitudes of the two types of nuclei are opposite in sign. The decrease may be calculated from the known coherent scattering amplitudes,  $b$ , by assuming random substitution by the solute atoms. The calculated relative

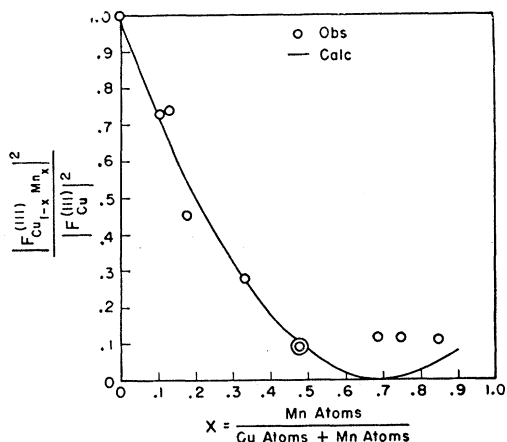


FIG. 3. Calculated and observed neutron structure factors for the (111) reflection of the copper-manganese alloys.

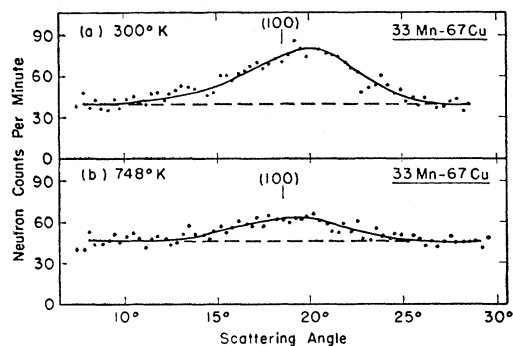


FIG. 4. Neutron diffraction patterns of the diffuse (100) reflection at (a) 300°K and (b) 748°K for the alloy 33 Mn-67 Cu.

<sup>9</sup> This pattern was obtained with a powdered, cylindrical specimen to insure randomness and using an improved neutron spectrometer and employing a higher flux reactor for greater line intensities.

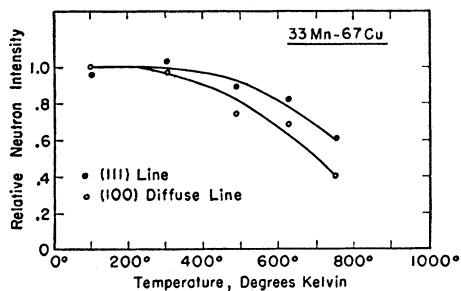


FIG. 5. Relative integrated intensities of the (100) diffuse reflection and the (111) reflection for the temperature range 100°K to 750°K of the alloy 33 Mn-67 Cu.

decrease of the normal reflections is then given by

$$\frac{I_x}{I_{Cu}} = \frac{|F_x|^2}{|F_{Cu}|^2} = \frac{[(1-x)b_{Cu} + xb_{Mn}]^2}{b_{Cu}^2}, \quad (1)$$

where

$$x = \frac{\text{Mn atoms}}{\text{Cu atoms} + \text{Mn atoms}}. \quad (2)$$

The calculated and observed relative intensities are given in Fig. 3. The calculated intensity in the region of 70 atomic percent manganese is zero. The observed finite intensity in this region is believed due to lack of perfect randomness and possible inhomogeneities in the samples.

The position of the broad (100) reflection is within the limits set by Ehrenfest's formula for the diffraction by two diffracting centers,  $\lambda = 2(0.8)d \sin\theta$  where  $d$  is the separation of the centers, and the Bragg formula,  $\lambda = 2d \sin\theta$ , where  $d$  is the atomic interplanar spacing. For the spacing equal to the lattice parameter  $a_0$  of the unit cell of the 67 Cu-33 Mn sample, the limits are  $0.8a_0 < d_{\text{observed}} < a_0$ , i.e., 2.98 Å < 3.27 Å < 3.72 Å. The size of the region having the periodicity responsible for the broad line was estimated to be of the order of 10 Å by applying the Scherrer equation for the broadening.

The effect of temperature on the form of the broad line is illustrated by Fig. 4. If it is assumed that the relative decrease in intensity of the broad line due to the usual Debye vibrations of the atoms is not greater than the observed relative decrease with temperature

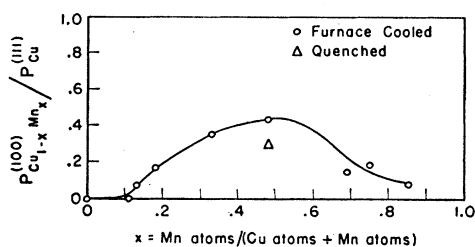


FIG. 6. Observed integrated neutron intensities of the diffuse (100) reflections of the copper-manganese alloys relative to the observed integrated intensity of the (111) reflection of copper.

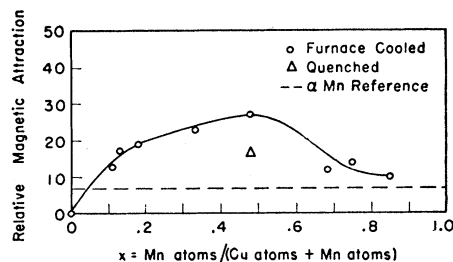


FIG. 7. Observed relative magnetic attraction of the copper-manganese alloys.

of the adjacent (111) normal reflection, then the more rapid decrease in intensity of the broad reflection, Fig. 5, may be attributed to a disordering of the short range crystal or magnetic ordering. Attempts to change the width of the maximum by annealing a few specimens at 750°C for three days was unsuccessful.

Generally the presence of a reflection in a neutron diffraction pattern and its absence in a corresponding x-ray pattern would indicate that the reflection is due to magnetic or antiferromagnetic coupling rather than atomic ordering.<sup>7</sup> In the present case of the broad neutron diffraction line, however, the correlation of the line with magnetic coupling cannot be so deduced because absence in the x-ray pattern may here be due to the closeness of the copper and manganese x-ray atomic scattering factors. That the intensity of the broad line is associated at least in part with magnetic ordering can be seen by the correlation of the observed integrated intensities of the line with the observed magnetic attractions of the samples as shown in Figs. 6 and 7. An attempt to detect the broad line in the 48 Mn-52 Cu sample by long x-ray exposures using Mn-filtered Fe  $K_{\alpha}$  radiation was not successful. From the relative exposures, however, it has been estimated that the contribution of crystal short-range ordering to the broad neutron peak is not greater than about  $\frac{1}{3}$ .

The neutron patterns of the Mn-rich samples exhibited lines at (110) and (201) positions in addition to the normal lattice lines. The neutron diffraction pattern of the alloy 85 Mn-15 Cu is shown in Fig. 2. The lines at (110) and (201) positions must arise from

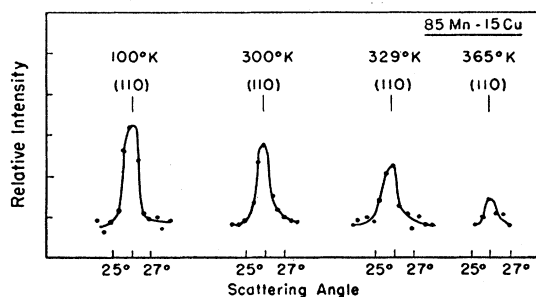


FIG. 8. The antiferromagnetic reflection of the alloy 85 Mn-15 Cu observed at various temperatures.

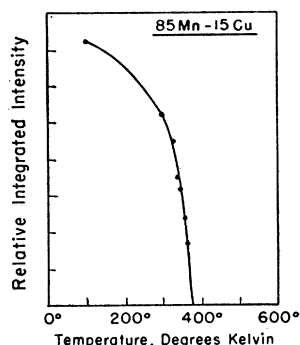


Fig. 9. Temperature dependence of the antiferromagnetic reflection of the alloy 85 Mn-15 Cu.

antiferromagnetic ordering of the atomic magnetic moments and not to atomic ordering of Cu and Mn on the face-centered tetragonal lattice, for if atomic ordering were responsible one would observe numerous additional superlattice lines in the Mn-rich alloys. The effect of temperature on the antiferromagnetic lines is shown in Fig. 8 for the (110) reflection of the alloy 85 Mn-15 Cu. Extrapolation of the intensity *versus* temperature curve of Fig. 9, gives a Néel temperature of about 380°K for this sample.

The presence of antiferromagnetism at Mn-rich compositions and the absence of superlattice lines due to atomic ordering suggest an antiferromagnetic structure based on the following considerations: In the manganese-rich samples the face-centered tetragonal crystal structure is similar to the high-temperature ( $\gamma$ ) form of manganese. The randomly distributed copper atoms then function to retain a lattice at room temperatures similar to the high-temperature  $\gamma$  form of pure manganese. Thus the observed antiferromagnetism would then arise from antiparallel couplings of the atomic magnetic moments of manganese on a face-centered tetragonal lattice.

The antiferromagnetic structure shown in Fig. 10 satisfies the observed presence and absence of antiferromagnetic lines. The manganese moments are parallel to the face-centered tetragonal  $c$  axis with the directions of the moments alternately pointed upward and downward at distances  $c_0/2$  along the  $c$  axis. The calculated and observed intensities of the antiferromagnetic reflections are given in Table II. The observed intensity of the diminished broad (100) reflection is taken to be zero, for this reflection is considered as the

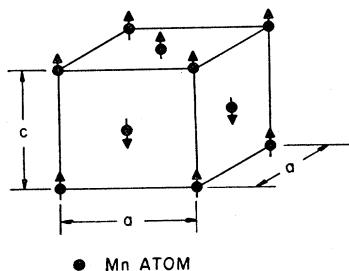


FIG. 10. Antiferromagnetic structure approached by the  $\gamma$  solid solution phase of copper-manganese alloys at large manganese compositions.

residue of the short-range magnetic ordering composition range.

The incoherent scattering in a neutron diffraction pattern generally consists of contributions from nuclear spin, isotope effect, thermal vibrations, and multiple scattering.<sup>4</sup> If the sample is paramagnetic, there is present also a paramagnetic incoherent scattering.<sup>8</sup> In the case of a random substitutional solid solution there should be in addition a contribution due to atomic randomness of the two atomic species on the lattice sites. The differential neutron scattering for the latter can be given by analogy with the corresponding quantity for x-rays by

$$d\sigma_R/d\Omega = x(1-x)(b_{Cu} - b_{Mn})^2. \quad (3)$$

Because of the opposite signs of  $b_{Cu}$  and  $b_{Mn}$  for the present binary alloy series, this component of incoherent scattering can be quite large.

The observed incoherent scattering in the near forward direction at room temperature is shown in Fig. 11. The multiple-scattering contribution was calculated from the tables prepared by Brockhouse.<sup>10</sup> The nuclear spin and isotope contribution was estimated

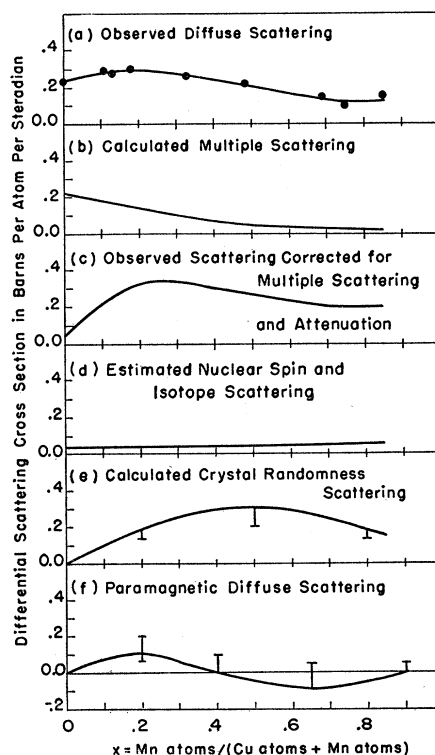


FIG. 11. Analysis of the observed diffuse neutron scattering at low angles ( $10^\circ$ ) at room temperature for the copper-manganese alloys. (The paramagnetic contribution (f) is estimated from the residue scattering after contributions from other effects are removed.)

<sup>10</sup> The authors are indebted to Dr. B. N. Brockhouse for the use of the tables in advance of publication.

by using the difference between the known total bound scattering cross sections of copper and manganese and their known coherent scattering cross sections. The crystal disorder scattering was calculated using Eq. (3) and can only be considered an upper limit because any short-range atomic ordering present will decrease the randomness contribution. The Debye thermal vibration contribution is not considered because it is negligible near zero scattering angle. After subtraction of the various estimated incoherent contributions, the residue is an estimate of the incoherent scattering due to randomly oriented atomic magnetic moments at room temperature. This paramagnetic scattering first increases by addition of paramagnetic manganese to copper. The gradual decrease following about 20 atomic percent manganese is largely due to the formation of the short-range magnetic ordering. At about 50 atomic percent, when the short-range magnetic ordering is greatest, the paramagnetic scattering is relatively small. The continued relatively small paramagnetic scattering at the still higher compositions is at least in part due to the transition into the antiferromagnetic structure at manganese-rich compositions. The negative values are due to data inaccuracies and overestimates in correcting for the various components of scattering, especially the crystal randomness component.

The analysis of the diffuse background is helpful in

TABLE II. Calculated and observed antiferromagnetic neutron diffraction intensities for 85 Mn-15 Cu alloy.

<i>hkl</i>	<i>J</i>	<i>F<sub>m</sub></i>	<i>d<sup>a</sup></i>	<i>f<sub>m</sub><sup>b</sup></i> ×10 <sup>12</sup>	<i>q<sup>2</sup></i>	<i>J F<sub>m</sub> <sup>2</sup>q<sup>2</sup></i>	Calc <sup>c</sup> <i>P/P<sub>110</sub></i>	Obs <i>P/P<sub>110</sub></i>
100	4	0					0.00	0.0
001	2	$\frac{4}{3}f_m$	3.64Å	0.76	0.00		0.00	0.0
110	4	$\frac{4}{3}f_m$	2.66	0.62	1.00	24.6	1.00	1.0
101	8	0					0.00	0.0
111	8	0					0.00	0.0
200	4	0					0.00	0.0
002	2	0					0.00	0.0
210	8	0					0.00	0.0
201	8	$\frac{4}{3}f_m$	1.67	0.26	0.81	7.0	0.28	0.2

<sup>a</sup> Spacings calculated from x-ray data of alloy 85 Mn-15 Cu.

<sup>b</sup> Magnetic structure factors taken from curve in reference 8.

<sup>c</sup> Debye-Waller temperature correction not applied.

interpretation of the observed diffuse scattering and of the correlated structures; however, the fact that the samples were not essentially in the paramagnetic state, together with errors in correcting for the various scattering components, prevent effective magnetic moments to be deduced.

#### ACKNOWLEDGMENTS

The authors wish to thank Dr. G. R. Ringo for stimulating discussions on the problem of multiple scattering and Professor P. L. Copeland for his interest through this investigation.

## Optical Absorption Band Edge in Anisotropic Crystals\*

G. DRESSELHAUS†

*Institute for the Study of Metals, University of Chicago, Chicago, Illinois*

(Received June 18, 1956)

The shape of the optical absorption band edge in insulating crystals is discussed for both direct and indirect electronic transitions. Selection rules are invoked to explain the apparent shift in the band edge with polarization observed in anisotropic crystals. The absorption coefficient obeys a law of the form  $K \propto (\hbar\omega - E)^n$ , where  $E$  is closely related to the minimum band gap and  $n$  is  $\frac{1}{2}$  for allowed direct transitions,  $\frac{3}{2}$  for forbidden direct transitions, and 2 for indirect transitions. The experimental observations of the shift in CdS and Te are analyzed in terms of conduction and valence band extrema at  $\mathbf{k}=0$  with symmetry types such that the transition is allowed for light polarization perpendicular to the hexagonal axis and forbidden for the polarization parallel to this axis.

### I. INTRODUCTION

IN recent years, the dependence of the electronic transport properties in insulators and semiconductors on the details of the energy band structure has been extensively studied both experimentally and theoretically. Phenomena such as cyclotron resonance, magnetoresistance, and elastoresistance have given an intimate knowledge of the band structure in a few

semiconductors. The purpose of this note is to point out how the optical properties of solids may provide additional information on the energy band structure.

In insulators the electrons or holes of importance in the transport processes are located near energy band extrema. A perturbation expansion (an expansion in powers of the electronic wave vector) about the extrema gives the dispersion relation, i.e.,  $E(\mathbf{k})$ , for electronic states in the neighborhood of the extrema. If the band extremum is nondegenerate, the dispersion relation is given by a power series expansion in the wave vector

\* Supported in part by the Office of Naval Research through a contract with the University of Chicago.

† Present address: Department of Physics, Cornell University, Ithaca, New York.

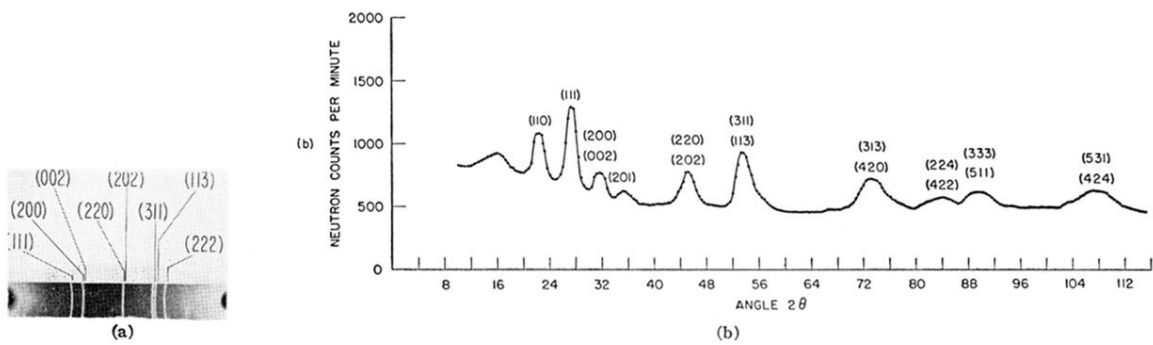


FIG. 2. Diffraction patterns of 85% Mn-15% Cu. (a) X-ray filtered Fe  $K_{\alpha}$  radiation, camera diameter 114.6 mm.  
 (b) Neutron,  $\lambda=1.01$  Å.